Communication

Holmium(III) Supermesityl-Imide Complexes Bearing Methylaluminato/Gallato Ligands

Dorothea Schädle [1], Cäcilia Maichle-Mössmer [1], Karl W. Törnroos [2] and Reiner Anwander [1,*]

[1] Institut für Anorganische Chemie, Universität Tübingen, Auf der Morgenstelle 18, 72076 Tübingen, Germany; E-Mails: dorothea.schaedle@uni-tuebingen.de (D.S.); Caecilia.Maichle-Moessmer@uni-tuebingen.de (C.M.-M.)

[2] Department of Chemistry, University of Bergen, Allégaten 41, 5007 Bergen, Norway; E-Mail: karl.tornroos@uib.no

* Author to whom correspondence should be addressed; E-Mail: reiner.anwander@uni-tuebingen.de; Tel.: +49-7071-29-72069; Fax: +49-7071-29-2436.

Academic Editors: Stephen Mansell and Steve Liddle

Abstract: Heterobimetallic μ_2-imide complexes $[Ho(\mu_2\text{-Nmes*})\{Al(CH_3)_4\}]_2$ (**1**, supermesityl = mes* = $C_6H_2tBu_3$-2,4,6) and $[Ho(\mu_2\text{-Nmes*})\{Ga(CH_3)_4\}]_2$ (**2**) have been synthesized from homoleptic complexes $Ho[M(CH_3)_4]_3$ (M = Al, Ga) via deprotonation of H_2Nmes* or with $K[NH(mes*)]$ according to a salt metathesis-protonolysis tandem reaction. Single-crystal X-ray diffraction of isostructural complexes $[Ho(\mu_2\text{-Nmes*})\{M(CH_3)_4\}]_2$ (M = Al, Ga) revealed asymmetric Ho_2N_2 metallacycles with very short Ho–N bond lengths and secondary Ho···arene interactions.

1. Introduction

The emerging field of rare-earth metal imide chemistry has revealed interesting structural motifs [1,2], but studies regarding their fundamental properties and reactivity are lagging behind. Bochkarev and Schumann were the first to report on a tetranuclear ytterbium(III) phenylimide complex obtainable via reduction of azobenzene by ytterbium naphthalenide [3]. Another synthesis strategy was developed by Evans *et al.*, adventitiously identifying $[Nd(NPh)(AlMe_2)(AlMe_4)_2]_2$ (Figure 1, **I**) via attempted

alkylation of [Nd(NHPh)₃(KCl)₃] with excess AlMe₃ [4]. We and others succeeded in the isolation of a series of rare-earth metal complexes (Figure 1, **II**–**III**, secondary interactions are not shown), by adopting the strategy of organoaluminum-assisted imide formation [5–10]. Similarly, deprotonation of lanthanide anilide complexes was achieved via treatment with butyllithium, affording complexes of type **IV** [11]. A different synthesis approach has been employed in the reactions of alkyl complexes with amine-boranes to yield Lewis acid (LA)-stabilized imido entities [Ln(NR)(BH₃)] (R = H, teraryl) [12,13].

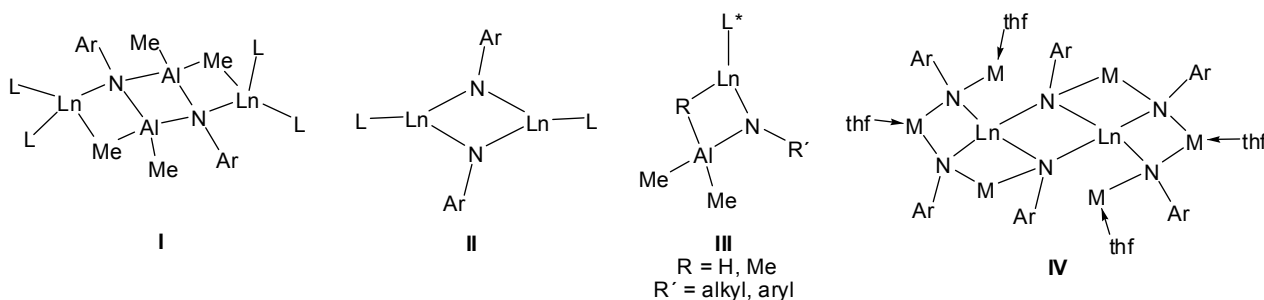**Figure 1.** Structural motifs of heterobimetallic rare-earth metal imide complexes: **I** (L = AlMe₄⁻, Ar = Ph), **II** (L = AlMe₃(NHAr)⁻, Ar = C₆H₃*i*Pr₂-2,6; L = AlMe₄⁻, Ar = C₆H₂*t*Bu₃-2,4,6), **III** (L* = monoanionic ancillary ligand), **IV** (M = Na, Li, Ar = C₆H₃*i*Pr₂-2,6).

In general, complexes of type [(L)Ln(NR)] or [(L)Ln(NR)(AlMe₃)] have shown promising usability in a range of areas, including catalytic cyclotrimerization of benzonitrile [14], synthesis of substituted pyridines [15], preparation of Ln/M heterobimetallics [16], hydroelementation reactions [17], and polymerization of dienes [18]. Further, such complexes give access to many different types of new Ln(III) imide complexes comprising alkyl-imide, amide-imide, alkoxide-imide, and cyclopentadienyl-imide compounds [18]. Moreover, derivatization of the Ln=N(R) functionality with small molecules and organic substrates revealed interesting reaction patterns and bonding features [19,20].

To fully investigate the implications of the choice of Ln(III) alkyl precursor for any envisioned synthesis, we also employed rare-earth metal tetramethylgallate complexes. Although the structural parameters of the Ln/M heterobimetalic complexes Ln[M(CH₃)₄]₃ (M = Al, Ga) [21–23] and the derived half-sandwich [24], metallocene [25], and scorpionate complexes [10,26,27] are similar, the reactivity, in some cases, is dramatically different [10,26,27]. For example, previous studies from our laboratory revealed that [(Tp*ᵗBu,Me*)Ln(CH₃)₂] (Tp*ᵗBu,Me* = hydrotris(3-*tert*-butyl-5-methylpyrazolyl)borate) and [(Tp*ᵗBu,Me*)Ln(CH₃){Ga(CH₃)₄}] gave the Ln(III) anilide complexes [(Tp*ᵗBu,Me*)Ln(CH₃)(NHR)] (R = alkyl, aryl), as opposed to the aluminum congener [(Tp*ᵗBu,Me*)Ln(CH₃){Al(CH₃)₄}], which yields complexes of type **III** [9,10].

While a series of dimeric LA-stabilized rare-earth metal imides (type **II**) has been reported previously [7], we now report on additional aniline-derived rare-earth metal imide complexes employing methylaluminate and methylgallate complexes. The intention was to investigate fundamental differences of organogallium *versus* organoaluminum moieties since GaMe₃ should behave as a weaker LA towards nitrogen than AlMe₃.

2. Results and Discussion

The μ2-imide complexes [Ln{Al(CH3)4}(μ2-Nmes*)]*x* (Ln = Y, La, Nd, Lu; mes* = C6H2*t*Bu3-2,4,6) were previously obtained from homoleptic heterobimetallic complexes Ln[Al(CH3)4]3 utilizing two distinct protocols: reaction with 2,4,6-tri-*tert*-butylaniline in *n*-hexane via methane elimination or with potassium (2,4,6-tri-*tert*-butylphenyl)amide in toluene according to a salt metathesis-protonolysis tandem reaction [7]. Similarly, the reaction of Ho[M(CH3)4]3 (M = Al, Ga) with H2Nmes* or K[NH(mes*)], respectively, led to dimeric complexes [Ho{M(CH3)4}(μ2-Nmes*)]2 (M = Al (**1**), Ga (**2**)) (Scheme 1). The identities of the holmium imide complexes **1** and **2** were confirmed by elemental analysis and single-crystal X-ray diffraction studies revealing isomorphous dimeric arrangements, featuring a Ho2N2 core on a crystallographic inversion center. The solid-state structures of **1** and **2** are depicted in Figure 2 with selected bond lengths and angles shown in Table 1. The geometry about the four-coordinate metal centers can best be described as distorted tetrahedral with two methyl groups and two imido nitrogen atoms at the four vertices. The rare-earth metal atoms are asymmetrically bridged by two μ2-imido nitrogen atoms, displaying one short (Ho–N, **1**: 2.107(1) Å; **2**: 2.102(3) Å) and one long contact (Ho–N, **1**: 2.283(1) Å; **2**: 2.288(3) Å). The Ho–N bond lengths in **1** and **2** are comparable to the distances in yttrium imide complexes, considering the similar ionic radii (Table 2).
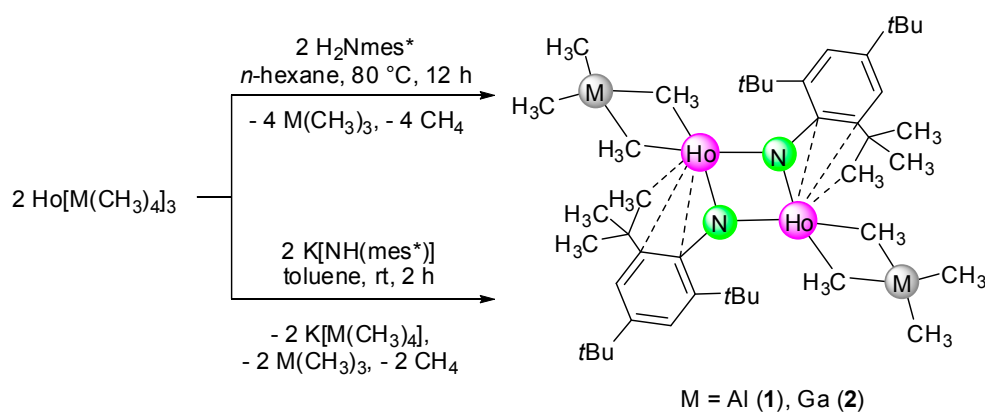
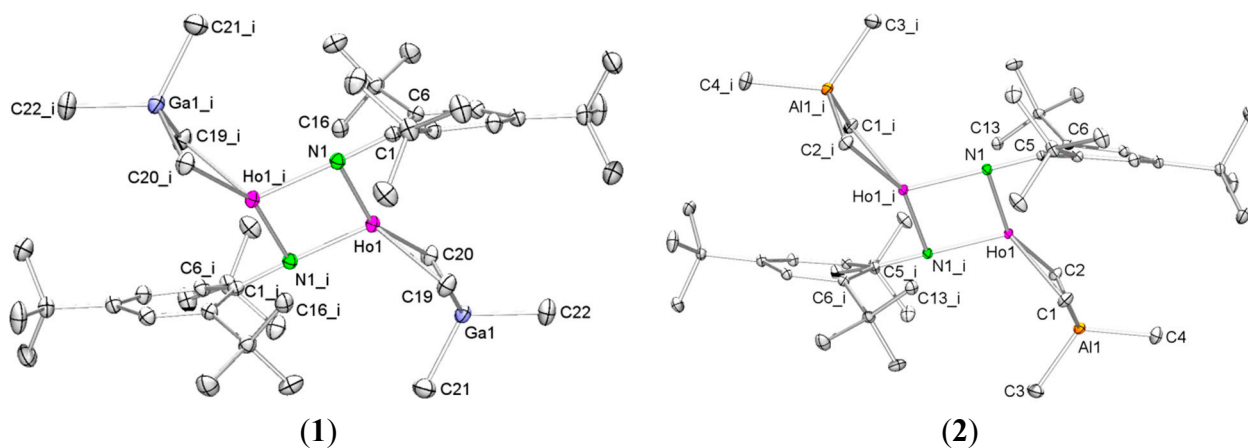

Scheme 1. Synthesis of holmium(III) imide complexes.

Figure 2. Solid-state structures of [Ho{Al(CH3)4}(μ2-Nmes*)]2 (**1**) and [Ho{Ga(CH3)4} (μ2-Nmes*)]2 (**2**) with 30% probability ellipsoids. Hydrogen atoms are omitted for clarity.

Table 1. Selected bond lengths [Å] and angles [°] of complexes **1** and **2**.

1		2	
Ho1–N1′	2.107(1)	Ho1–N1′	2.102(3)
Ho1–N1	2.283(1)	Ho1–N1	2.288(3)
Ho1′–N1	2.107(1)	Ho1′–N1	2.102(3)
Ho1–C1	2.512(2)	Ho1–C19	2.512(4)
Ho1–C2	2.598(2)	Ho1–C20	2.594(5)
Ho1–C5	2.626(1)	Ho1–C1	2.629(3)
Ho1–C6	2.715(1)	Ho1–C6	2.750(3)
Ho1–C13	2.833(1)	Ho1–C16	2.864(3)
Ho1···Al1	3.0838(5)	Ho1···Ga1	3.0573(4)
Al1–C1	2.0836(16)	Ga1–C19	2.115(4)
Al1–C2	2.0718(16)	Ga1–C20	2.092(4)
Al1–C3	1.9681(19)	Ga1–C21	1.978(4)
Al1–C4	1.9727(17)	Ga1–C22	1.974(4)
N1–C5	1.3811(18)	N1–C1	1.386(4)
N1′–Ho1–N1	84.63(4)	N1′–Ho1–N1	84.68(11)
Ho1′–N1–Ho1	95.37(4)	Ho1′–N1–Ho1	95.32(11)
Ho1′–N1–C5	175.67(10)	Ho1′–N1–C1	176.8(2)
Ho1–N1–C5	87.95(8)	Ho1–N1–C1	87.80(18)
C1–Ho1–C2	82.76(5)	C19–Ho1–C20	83.98(14)
C1–Al1–C2	108.80(6)	C19–Ga1–C20	108.63(15)
C3–Al1–C4	118.82(8)	C21–Ga1–C22	117.5(2)
C1–Ho1–C2–Al1	−11.34(5)	C19–Ho1–C20–Ga1	14.20(14)

Table 2. Selected Y–N(imido) and Ho–N(imido) bond lengths [Å].

Compounds	Ln–N	CN [a]	Reference
[(Tp$^{t\text{Bu,Me}}$)Y{NC$_6$H$_3$(CH$_3$)$_2$-2,6}(AlMe$_3$)] [c]	2.123(2)–2.128(3)	5	[10]
[(Tp$^{t\text{Bu,Me}}$)Y{NC$_6$H$_3$(CH$_3$)$_2$-2,6}(HAlMe$_2$)] [c]	2.133(2)	5	[8]
[(Tp$^{t\text{Bu,Me}}$)Y(NtBu)(AlMe$_3$)] [c]	2.081(3)–2.088(3)	5	[9]
[(Tp$^{t\text{Bu,Me}}$)Ho(NtBu)(AlMe$_3$)] [c]	2.083(2)–2.084(2)	5	[9]
[(Tp$^{t\text{Bu,Me}}$)Y(NAd)(AlMe$_3$)] [c,d]	2.092(2)–2.099(2)	5	[9]
[(Tp$^{t\text{Bu,Me}}$)Ho(NAd)(AlMe$_3$)] [c,d]	2.087(2)–2.090(2)	5	[9]
[(Tp$^{t\text{Bu,Me}}$)Y{NC$_6$H$_3$(CH$_3$)$_2$-2,6}(DMAP) [c,e]	2.024(4)	5	[10]
[(C$_5$Me$_4$SiMe$_3$)$_4$Y$_4$(μ_3-NCH$_2$CH$_3$)$_2$(μ_2-NCHPh)$_4$]	2.116(6)–2.418(6)	6/7	[14]
[L$_3$Y$_3$(μ_2-CH$_3$)$_3$(μ_3-CH$_3$)(μ_3-NR)] [f]	2.308(3)–2.435(7)	6	[28]
[Y{Al(CH$_3$)$_4$}(μ_2-Nmes*)]$_2$	2.1089(9)–2.2909(9)	6	[7]
[Ho{Al(CH$_3$)$_4$}(μ_2-Nmes*)]$_2$	2.107(1)–2.283(1)	6	[b]
[Ho{Ga(CH$_3$)$_4$}(μ_2-Nmes*)]$_2$	2.102(3)–2.288(3)	6	[b]

[a] CN = coordination number; [b] this work; [c] Tp$^{t\text{Bu,Me}}$ = hydrotris(3-*tert*-butyl-5-methylpyrazolyl)borate; [d] Ad = 1-adamantyl; [e] DMAP = 4-(dimethylamino)pyridine; [f] L = [PhC(NC$_6$H$_3$$iPr_2$-2,6)$_2$]$^-$; R = alkyl, aryl.

The pronounced asymmetry of the Ho$_2$N$_2$ core most likely originates from secondary interactions between the holmium centers and the *ipso* and *ortho* carbons as well as one CH$_3$ *tert*-butyl group of the bridging μ_2-Nmes* ligands. One distinct difference between [Ho{Al(CH$_3$)$_4$}(μ_2-Nmes*)]$_2$ (**1**) and

[Ho{Ga(CH$_3$)$_4$}(μ_2-Nmes*)]$_2$ (**2**) is the bending of the M(CH$_3$)$_4$ moiety being slightly more pronounced for the gallium derivative, since the softer Ga(III) center can achieve shorter Ln(III)···Ga(III) contacts.

A preliminary reactivity study of yttrium congener [Y{Al(CH$_3$)$_4$}(μ_2-Nmes*)]$_2$ [7] was performed in order to assess the feasibility of exchanging the AlMe$_4^-$ ligand by other ancillary ligands. The reaction of [Y{Al(CH$_3$)$_4$}(μ_2-Nmes*)]$_2$ with KCp* (Cp* = C$_5$Me$_5$) in toluene at 80 °C led to the formation of an off-white solid, which is insoluble in *n*-hexane and toluene. The ^{1}H NMR spectrum of the product indicated the formation of [Cp*Y(Nmes*)]$_n$. However, as shown previously, toluene-soluble imide complexes [(AlMe$_4$)Ln(NC$_6$H$_3$iPr-2,6)(AlMe$_3$)$_x$]$_2$ readily undergo salt-metathesis reactions with a variety of alkaline metal salts [M^I(L)] (L = silylamide, cyclopentadienyl, aryloxide) to generate heteroleptic Ln(III) imide complexes [18].

3. Experimental Section

3.1. General Procedures

All operations were performed with rigorous exclusion of air and water, using standard Schlenk, high-vacuum, and glovebox techniques (MBraun MBLab; <1 ppm O$_2$, <1 ppm H$_2$O). Toluene and *n*-hexane were purified by using Grubbs columns (MBraun SPS, solvent purification system, MBraun, Garching, Germany) and stored in a glovebox; [D$_6$]benzene was obtained from Aldrich (St. Louis, MO, USA), degassed, dried over Na for 24 h, and filtered. Then 2,4,6-tri-*tert*-butylaniline was obtained from Aldrich and used as received. Potassium (2,4,6-tri-*tert*-butylphenyl)amide was synthesized according to literature procedures [7]. Homoleptic complexes [Ho{Al(CH$_3$)$_4$}$_3$] [22,29] and [Ho{Ga(CH$_3$)$_4$}$_3$] [30,31] (**2**) were prepared according to literature methods. DRIFT spectra were recorded on a NICOLET 6700 FTIR spectrometer (Thermo Scientific, Dreieich, Germany) using dried KBr and KBr window. Elemental analyses were performed on an Elementar Vario Micro Cube (Elementar, Hanau, Germany).

3.2. [Ho{M(CH$_3$)$_4$}(μ_2-Nmes*)]$_2$ (1 and 2)

3.2.1. Procedure A

A solution of Ho[M(CH$_3$)$_4$]$_3$ in toluene (3 mL) was added to a vigorously stirred suspension of potassium (2,4,6-tri-*tert*-butylphenyl)amide in toluene (2 mL). The reaction mixture was stirred for 2 h at ambient temperature and the toluene solution then separated by centrifugation, decanted, and filtrated. The solid residue (product and K[M(CH$_3$)$_4$] was extracted with additional toluene (5 × 2 mL). The extract was dried under vacuum and triturated with *n*-hexane (2 × 2 mL). After that the solid was washed with *n*-hexane (2 × 2 mL), followed by drying under reduced pressure. Compounds **1** and **2** were obtained as powder or by crystallization from the mother liquor at ambient temperature.

3.2.2. Procedure B

A solution of 2,4,6-tri-*tert*-butylaniline in *n*-hexane (3 mL) was added to a solution of Ho[M(CH$_3$)$_4$]$_3$ in *n*-hexane (2 mL). The reaction mixture was stirred for 8 h at 80 °C. The solution turned orange and a precipitate was formed. The mixture was chilled to ambient temperature, the solid product was

separated by centrifugation and washed with *n*-hexane (2 × 2 mL). The procedure was repeated twice with the combined extracts. Compounds **1** and **2** were dried *in vacuo* and obtained as orange powder.

3.3. [Ho{Al(CH₃)₄}(μ₂-Nmes*)]₂ (1)

3.3.1. Procedure A

Following the procedure described above, $Ho[Al(CH_3)_4]_3$ (85.3 mg, 0.20 mmol) and potassium(2,4,6-tri-*tert*-butylphenyl)amide (59.9 mg, 0.20 mmol) yielded $[Ho\{Al(CH_3)_4\}(\mu_2\text{-Nmes*})]_2$ as orange crystals (102.3 mg, 0.10 mmol, ≥99%).

3.3.2. Procedure B

Following the procedure described above, $Ho[Al(CH_3)_4]_3$ (85.3 mg, 0.20 mmol) and 2,4,6-tri-*tert*-butylaniline (52.3 mg, 0.20 mmol) yielded $[Ho\{Al(CH_3)_4\}(\mu_2\text{-Nmes*})]_2$ as orange powder (38.4 mg, 0.04 mmol, 40%).

3.3.3. Physical Data of **1**

DRIFT IR (KBr): 3014 w, 2962 s, 2869 m, 2773 w, 1588 w, 1477 w, 1462 w, 1394 m, 1377 m, 1361 m, 1340 w, 1274 m, 1244 s, 1227 m, 1200 s, 1108 w, 916 w, 894 w, 874 w, 856 m, 783 w, 755 w, 716 s, 694 vs, 663 w, 638 w, 609 w, 578 m, 547 w, 504 m, 476 w, 458 w, 437 m·cm^{-1}; elemental analysis calcd (%) for $C_{44}H_{82}Al_2N_2Ho_2$ (1022.96 g·mol^{-1}): C 51.66, H 8.08, N 2.74; found: C 51.76, H 7.84, N 2.74.

3.4. [Ho(GaMe₄)(μ₂-Nmes*)]₂ (2)

3.4.1. Procedure A

Following the procedure described above, $Ho[Ga(CH_3)_4]_3$ (269.9 mg, 0.47 mmol) and potassium(2,4,6-tri-*tert*-butylphenyl)amide (139.9 mg, 0.47 mmol) yielded $[Ho\{Ga(CH_3)_4\}(\mu_2\text{-Nmes*})]_2$ as orange crystals (520.1 mg, 0.47 mmol, ≥99%).

3.4.2. Procedure B

Following the procedure described above, $Ho[Ga(CH_3)_4]_3$ (236.7 mg, 0.43 mmol) and 2,4,6-tri-*tert*-butylaniline (127.9 mg, 0.43 mmol) yielded $[Ho\{Ga(CH_3)_4\}(\mu_2\text{-Nmes*})]_2$ as orange powder (100.8 mg, 0.09 mmol, 42%).

3.4.3. Physical Data of **2**

DRIFT IR (KBr): 2962 vs, 2904 m, 2869 m, 2774 w, 1588 vw, 1477 w, 1460 w, 1394 s, 1378 m, 1360 m, 1274 m, 1246 vs, 1227 m, 1193 m, 1109 w, 915 vw, 875 w, 856 s, 783 w, 755 w, 716 w, 662 vw, 594 w, 556 w, 530 w, 505 m, 476 vw, 428 w·cm^{-1}; elemental analysis calcd for $C_{44}H_{82}Ga_2N_2Ho_2$ (1108.44 g/mol): C 47.68, H 7.46, N 2.53; found: C 47.91, H 7.42, N 2.52.

3.5. X-Ray Crystallography

Crystal data for compounds **1** and **2** are given in Table 3. Bond lengths and angles are listed in Table 2. Crystals of **1** and **2** were grown using standard techniques from saturated toluene solutions. Suitable single crystals for X-ray structure analyses were selected in a glovebox and coated with Parabar 10312 and fixed on a nylon loop/glass fiber.

Table 3. Crystallographic data for compounds **1** and **2**.

	1	2
Formula	$C_{44}H_{82}Al_2Ho_2N_2$	$C_{44}H_{82}Ga_2Ho_2N_2$
Color	Yellow	Yellow
M_r (g·mol^{-1})	1022.94	1108.41
Cryst system	Monoclinic	Triclinic
Space group	$C2/c$	$P\overline{1}$
a [Å]	24.0888(13)	10.1896(4)
b [Å]	11.7687(6)	11.5565(5)
c [Å]	20.4327(11)	11.5966(5)
α [°]	90	65.090(3)
β [°]	111.5590(10)	83.184(3)
γ [°]	90	84.962(4)
V [Å^3]	5387.3(5)	1228.69(9)
Z	4	1
F(000)	2080	556
T [K]	103(2)	173(2)
ρ_{calcd} (g cm^3)	1.261	1.498
μ(mm^{-1})	2.974	4.297
R$_1$ (obsd.) [a]	0.0172	0.0296
wR$_2$ (all) [b]	0.0466	0.0661
S [c]	1.042	1.082

[a] $R_1 = \Sigma(||F_0| - |F_c||)/\Sigma|F_0|$, $F_0 > 4\sigma(F_0)$; [b] $wR_2 = \{\Sigma[w(F_0^2 - F_c^2)^2/\Sigma[w(F_0^2)^2]\}^{1/2}$; [c] $S = [\Sigma w(F_0^2 - F_c^2)^2/(n_0 - n_p)]^{1/2}$.

Data for compound **2** were collected on a Stoe IPDS 2T instrument equipped with a fine focus sealed tube and graphite monochromator using MoK$_\alpha$ radiation (λ = 0.71073 Å) performing ω scans. Raw data were collected and integrated using Stoe's X-Area software package [32]. A numerical absorption correction based on crystal shape optimization was applied using Stoe's X-Red [33] and X-Shape [34]. X-ray data for compound **1** were collected on a Bruker AXS, TXS rotating anode instrument using a Pt^{135} CCD detector, and graphite monochromated using MoK$_\alpha$ radiation (λ = 0.71073 Å), employing ω-scans. Raw data were processed using APEX [35] and SAINT [36], corrections for absorption effects were applied using SADABS [37]. The structure was solved by direct methods and refined against all data by full-matrix least-squares methods on F^2 using SHELXTL [38] and ShelXle [39]. All graphics were produced employing ORTEP-3 [40] and POV-Ray [41]. Further details of the refinement and crystallographic data are listed in the CIF files. CCDC 1426090 (**1**) and 1426091 (**2**) contain all the supplementary crystallographic data for this paper. These data can be obtained free of charge from The Cambridge Crystallographic Data Centre via www.ccdc.cam.ac.uk/data_request/cif.

4. Conclusions

Like the homoleptic tetramethylaluminate $Ho[Al(CH_3)_4]_3$, the respective gallate complex can be converted into imido-bridged complexes $[Ho\{M(CH_3)_4\}(\mu_2\text{-Nmes*})]_2$ (M = Al (**1**), Ga (**2**)). Depending on the synthesis protocol, meaning either protonolysis or the salt metathesis-protonolysis tandem reaction, the imide complexes are formed in moderate to excellent yields, respectively. Preliminary experiments on the capability of $[Ln\{Al(CH_3)_4\}(\mu_2\text{-Nmes*})]_2$ to engage in ligand exchange reactions were hampered by solubility issues. Ongoing studies in our group address the feasibility of imide-tetramethylgallate complexes derived from other primary amines/anilines. We have recently shown that switching to the H_2Ndipp (dipp = $C_6H_3iPr_2$-2,6) proligand significantly enhanced the solubility of the isolated bimetallic rare-earth metal imide complexes $Ln_2(\mu_2\text{-Ndipp})(\mu_3\text{-Ndipp})[(\mu_2\text{-}CH_3)_2Al(CH_3)][Al(CH_3)_4]_2$, thus allowing for facile derivatization [18].

Supplementary Materials

Supplementary materials can be found at http://www.mdpi.com/2304-6740/3/4/0500/s1.

Acknowledgments

Author Contributions

All reactions and analyses described were planned and conducted by Dorothea Schädle. Analyses include DRIFT spectroscopy and elemental analysis. Publication writing was done by Dorothea Schädle and Reiner Anwander. The structural analyses by single crystal X-ray diffraction were performed by Cäcilia Maichle-Mössmer and Karl W. Törnroos.

Conflicts of Interest

The authors declare no conflict of interest.

References

1. Giesbrecht, G.R.; Gordon, J.C. Lanthanide alkylidene and imido complexes. *Dalton Trans.* **2004**, 2387–2393, doi:10.1039/B407173E.
2. Summerscales, O.T.; Gordon, J.C. Complexes containing multiple bonding interactions between lanthanoid elements and main-group fragments. *RSC Adv.* **2013**, *3*, 6682–6692.
3. Trifonov, A.A.; Bochkarev, M.N.; Schumann, H.; Loebel, J. Reduction of azobenzene by naphthaleneytterbium: A tetranuclear ytterbium(III) complex combining 1,2-diphenylhydrazido(2−) and phenylimido ligands. *Angew. Chem. Int. Ed. Engl.* **1991**, *30*, 1149–1151.
4. Evans, W.J.; Ansari, M.A.; Ziller, J.W.; Khan, S.I. Utility of arylamido ligands in yttrium and lanthanide chemistry. *Inorg. Chem.* **1996**, *35*, 5435–5444.

5. Gordon, J.C.; Giesbrecht, G.R.; Clark, D.L.; Hay, P.J.; Keogh, D.W.; Poli, R.; Scott, B.L.; Watkin, J.G. The first example of a μ_2-imido functionality bound to a lanthanide metal center: X-ray crystal structure and DFT study of [(μ-ArN)Sm(μ-NHAr)(μ-Me)AlMe$_2$]$_2$ (Ar = 2,6-^{i}Pr$_2$C$_6$H$_3$). *Organometallics* **2002**, *21*, 4726–4734.

6. Scott, J.; Basuli, F.; Fout, A.R.; Huffmann, J.C.; Mindiola, D.J. Evidence for the existence of a terminal imidoscandium compound: Intermolecular C–H activation and complexation reactions with the transient Sc–NAr species. *Angew. Chem. Int. Ed.* **2008**, *47*, 8502–8505.

7. Schädle, D.; Schädle, C.; Törnroos, K.W.; Anwander, R. Organoaluminum-assisted formation of rare-earth metal imide complexes. *Organometallics* **2012**, *31*, 5101–5107.

8. Schädle, C.; Schädle, D.; Eichele, K.; Anwander, R. Methylaluminum-supported rare-earth-metal dihydrides. *Angew. Chem. Int. Ed.* **2013**, *52*, 13238–13242.

9. Schädle, D.; Maichle-Mössmer, C.; Schädle, C.; Anwander, R. Rare-earth-metal methyl, amide, and imide complexes supported by a superbulky scorpionate ligand. *Chem. Eur. J.* **2014**, *21*, 662–670.

10. Schädle, D.; Meermann-Zimmermann, M.; Schädle, C.; Maichle-Mössmer, C.; Anwander, R. Rare-earth metal complexes with terminal imido ligands. *Eur. J. Inorg. Chem.* **2015**, 1334–1339.

11. Chan, H.S.; Li, H.W.; Xie, Z. Synthesis and structural characterization of imido–lanthanide complexes with a metal–nitrogen multiple bond. *Chem. Commun.* **2002**, 652–653, doi:10.1039/B110793C.

12. Li, J.; Gao, D.; Hu, H.; Cui, C. Reaction of a bulky amine borane with lanthanide trialkyls. Formation of alkyl lanthanide imide complexes. *New J. Chem.* **2015**, *39*, 7567–7570.

13. Rad'kov, V.; Dorcet, V.; Carpentier, J.F.; Trifonov, A.; Kirillov, E. Alkylyttrium complexes of amidine–amidopyridinate ligands. Intramolecular C(sp^3)–H activation and reactivity studies. *Organometallics* **2013**, *32*, 1517–1527.

14. Cui, D.; Nishiura, M.; Hou, Z. Lanthanide-imido complexes and their reactions with benzonitrile. *Angew. Chem. Int. Ed.* **2005**, *44*, 959–962.

15. Wicker, B.F.; Scott, J.; Fout, A.R.; Pink, M.; Mindiola, D.J. Atom-economical route to substituted pyridines via a scandium imide. *Organometallics* **2011**, *30*, 2453–2456.

16. Lu, E.; Zhou, Q.; Li, Y.; Chu, J.; Chen, Y.; Leng, X.; Sun, J. Reactivity of scandium terminal imido complexes towards metal halides. *Chem. Commun.* **2012**, *48*, 3403–3405.

17. Chu, J.; Lu, E.; Chen, Y.; Leng, X. Reversible addition of the Si–H bond of phenylsilane to the Sc=N bond of a scandium terminal imido complex. *Organometallics* **2012**, *32*, 1137–1140.

18. Schädle, D.; Schädle, C.; Schneider, D.; Maichle-Mössmer, C.; Anwander, R. Versatile Ln$_2$(μ-NR)$_2$-imide platforms for ligand exchange and isoprene polymerization. *Organometallics* **2015**, *34*, 4994–5008.

19. Chu, J.; Lu, E.; Liu, Z.; Chen, Y.; Leng, X.; Song, H. Reactivity of a scandium terminal imido complex towards unsaturated substrates. *Angew. Chem. Int. Ed.* **2011**, *50*, 7677–7680.

20. Chu, J.; Han, X.; Kefalidis, C.E.; Zhou, J.; Maron, L.; Leng, X.; Chen, Y. Lewis acid triggered reactivity of a Lewis base stabilized scandium-terminal imido complex: C–H bond activation, cycloaddition, and dehydrofluorination. *J. Am. Chem. Soc.* **2014**, *136*, 10894–10897.

21. Evans, W.J.; Anwander, R.; Doedens, R.J.; Ziller, J.W. The use of heterometallic bridging moieties to generate tractable lanthanide complexes of small ligands. *Angew. Chem. Int. Ed. Engl.* **1994**, *33*, 1641–1644.

22. Zimmermann, M.; Frøystein, N.Å.; Fischbach, A.; Sirsch, P.; Dietrich, H.M.; Törnroos, K.W.; Herdtweck, E.; Anwander, R. Homoleptic rare-earth metal (III) tetramethylaluminates: Structural chemistry, reactivity, and performance in isoprene polymerization. *Chem. Eur. J.* **2007**, *13*, 8784–8800.

23. Dietrich, H.M.; Raudaschl-Sieber, G.; Anwander, R. Trimethylyttrium and trimethyllutetium. *Angew. Chem. Int. Ed.* **2005**, *44*, 5303–5306.

24. Dietrich, H.M.; Maichle-Mössmer, C.; Anwander, R. Donor-assisted tetramethylaluminate/gallate exchange in organolanthanide complexes: Pushing the limits of Pearson's HSAB concept. *Dalton Trans.* **2010**, *39*, 5783–5785.

25. Dietrich, H.M.; Törnroos, K.W.; Herdtweck, E.; Anwander, R. Tetramethylaluminate and tetramethylgallate coordination in rare-earth metal half-sandwich and metallocene complexes. *Organometallics* **2009**, *28*, 6739–6749.

26. Zimmermann, M.; Takats, J.; Kiel, G.; Törnroos, K.W.; Anwander, R. Ln(III) methyl and methylidene complexes stabilized by a bulky hydrotris(pyrazolyl)borate ligand. *Chem. Commun.* **2008**, 612–614.

27. Zimmermann, M.; Litlabø, R.; Törnroos, K.W.; Anwander, R. "Metastable" Lu(GaMe$_4$)$_3$ reacts like masked [LuMe$_3$]: Synthesis of an unsolvated lanthanide dimethyl complex. *Organometallics* **2009**, *28*, 6646–6649.

28. Hong, J.; Zhang, L.; Wang, K.; Zhang, Y.; Weng, L.; Zhou, X. Methylidene rare-earth-metal complex mediated transformations of C=N, N=N and N–H bonds: New routes to imido rare-earth-metal clusters. *Chem. Eur. J.* **2013**, *19*, 7865–7873.

29. Evans, W.J.; Anwander, R.; Ziller, J.W. Inclusion of Al$_2$Me$_6$ in the crystalline lattice of the organometallic complexes LnAl$_3$Me$_{12}$. *Organometallics* **1995**, *14*, 1107–1109.

30. Dietrich, H.M.; Meermann, C.; Törnroos, K.W.; Anwander, R. Sounding out the reactivity of trimethylyttrium. *Organometallics* **2006**, *25*, 4316–4321.

31. Zimmermann, M.; Rauschmaier, D.; Eichele, K.; Törnroos, K.W.; Anwander, R. Amido-stabilized rare-earth metal mixed methyl methylidene complexes. *Chem. Commun.* **2010**, *46*, 5346–5348.

32. X-Area v. 1.55; Stoe & Cie GmbH: Darmstadt, Germany, 2009.

33. X-Red 32 v. 1.53; Stoe & Cie GmbH: Darmstad, Germany, 2009.

34. X-Shape v.2.12.2; Stoe & Cie GmbH: Darmstadt, Germany, 2009.

35. APEX v. 2012.10_0; Bruker AXS Inc.: Madison, WI, USA, 2012.

36. SAINT v. 7.99A; Bruker AXS Inc.: Madison, WI, USA, 2012.

37. Sheldrick, G.M. SADABS v. 2012/1; Bruker AXS Inc.: Madison, WI, USA, 2012.

38. Sheldrick, G.M. Crystal structure refinement with *SHELXL. Acta Crystallogr. Sect. C* **2015**, *71*, 3–8.

39. Hübschle, C.B.; Sheldrick, G.M.; Dittrich, B. *ShelXle*: A Qt graphical user interface for *SHELXL. J. Appl. Crystallogr.* **2011**, *44*, 1281–1284.

40. Farrugia, L.J. *WinGX* and *ORTEP* for *Windows*: An update. *J. Appl. Crystallogr.* **2012**, *45*, 849–854.

41. POV-Ray v. 3.7; Persistence of Vision Pty. Ltd.: Williamstown, Australia, 2004. Available online: http://www.povray.org/ (accessed on 18 March 2014).